μFLU12-2012/24

NUMERICAL ANALYSIS OF HEAT TRANSFER CHARACTERISTICS OF COMBINED ELECTROOSMOTIC AND PRESSURE-DRIVEN FULLY DEVELOPED FLOW OF POWER LAW NANOFLUIDS IN MICROCHANNELS

Anindya Aparajita, Ashok K. Satapathy*[1]
[1]Department of Mechanical Engineering, National Institute of Technology, Rourkela, Odisha, India
anindya.rkl@gmail.com, aksatapathy2010@gmail.com

KEY WORDS

Microchannel, nanofluid, electroosmotic, pressure driven, viscous dissipation, Joule heating, non-newtonian (power law) fluid, electric double layer

ABSTRACT

Thermal transport characteristics of combined electroosmotic and pressur-driven flow of non-Newtonian (power-law) nanofluids through a microchannel have been studied. Non-Newtonian fluids can influence the thermal behaviour of the flow by affecting the rate of heat convection and viscous dissipation. Electroosmotic phenomenon causes resistance heating of the fluid, called Joule heating. Joule heating becomes a note-worthy phenomenon in microscale flow dynamics as the thickness of the ionic charged layer or electric double layer (EDL) is only about one-tenth to one-hundredth of the channel height. Nanofluids are known to have better heat transfer characteristics than conventional fluids at microscale. A complete parametric study has been carried out to investigate the effect of different flow and electrolytic parameters on the thermal behaviour of the flow. The governing equations have been solved semi-analytically under constant wall heat flux condition taking into account the effects of viscous dissipation and Joule heating. Power-law fluids of both shear-thinning and shear-thickening nature have been considered. The governing equations have been solved only for hydrodynamically and thermally fully-developed flow. Three nanofluidic parameters have been taken into consideration, namely: viscosity, electrical permittivity and electrical resistivity. These parameters have been introduced as ratios with reference to the corresponding properties of a conventional fluid.

1. INTRODUCTION

The increasing miniaturization of electronic components has led to an increased interest in microscale heat transfer. The concept of integrating heat sinks into the electronic chip's matrix is alluring but has complex operational and fabrication-oriented challenges. This has led to a considerable amount of research in this arena to simplify operation and fabrication, and to increase the effectiveness of heat transfer at the same time. In this work, the emphasis has been laid on flow of liquids through microchannels under constant wall heat flux condition taking into account the effects of viscous dissipation and Joule heating. When an electrolyte flows through a microtube or microchannel, the walls get charged on contact with the fluid. This causes a change in the ionic distribution of the fluid [1]. By applying electric field, the bulk motion of the ions and thus the fluid, can be achieved. This phenomenon is called electroosmosis [2]. Electroosmotic flow is characterized by Joule Heating which arises due the fluid electrical resistivity and the applied electric field. Maynes and Webb [3] were the first to consider the thermal aspects of electroosmotic flow. They analytically studied the convective transport for a parallel plate microchannel and circular microtube under constant heat flux and constant wall temperature condition for fully-developed region. Liechty et al. [4] extended this work for high zeta potential conditions.

Fluid flow through microchannel can be further assisted by the combined effect of electroosmosis and pressure gradient. Chen [5] studied the thermal transport characteristics of combined electroosmotic and

* Corresponding author

pressure driven flows taking Joule heating and temperature dependent properties into account. Sadeghi and Saidi [6] developed analytical solutions for mixed electroosmotic and pressure driven flows in slit microchannels taking viscous dissipation into consideration.

The study of electroosmotic flows for non-Newtonian fluids is comparatively new as is evident from the small number of literature available. The electroosmotic capillary transport of power-law fluids in rectangular microchannel has been studied by Chakraborty [7] by means of semi-analytical mathematical model. Zhao et al.. [8] gave an approximate analytical solution based on Debye-Hückel approximation for velocity profile of power law fluid in a slit microchannel. The electroviscous effects of pressure driven power law fluids in through circular microtube for fully-developed flow conditions has been numerically investigated by Bharti et al. [9]. Vasu and De [10] studied the electrokinetic effects in steady, fully-developed pressure driven flow of power law fluids using Debye-Hückel approximation for slit microchannels. Numerical investigation of combined flow of power law fluids in slit microchannel was carried out by Babie et al. [11]. Das and Chakraborty [12] were the first to analyze the thermal transport characteristics of electroosmotic flow of power law fluids. Sadeghi et al. [13] and Chen [14] provided the temperature profile and Nusselt number associated with electro-osmotic flow of non-Newtonian power law fluids based on Debye Hückel linearization. They used two different approaches for the same. Babaie et al. [15] conducted a complete parametric study to analyse the effects of flow behavior index, velocity scale ratio, dimensionless Debye Hückel parameter, Joule heating and viscous dissipation parameters on the thermal features of mixed electroosmotic and pressure driven flow of power law fluids.

The trend for using stable suspension of nano-particles in a fluid medium is growing. Known as nanofluids, these suspensions possess high effective transport coefficients owing to random movement of nano-particles, molecular level layering of liquids at liquid-particle interfaces, ballistic phonon transport through particles and nano particle clustering [16-17]. Hung [18] analyzed the forced convection of nano-fluids with viscous dissipation in microchannels. Jang and Choi [19] investigated the cooling performance of microchannel heat sinks with nanofluids, by employing a model for thermal conductivity that is influenced by Brownian motion of the nanoparticles. Chakraborty and Roy [20] investigated the cooling performance of thermally developing electroosmotic flow of nanofluid without considering imposed pressure gradients.

The current work is an extension of the work of Babaie et al. [15] to determine the heat transfer characteristics of mixed pressure and electroosmotically driven flow for power law electrolyte based nanofluids in the fully-developed region. It has been shown that the changes in heat transfer can be visualized by inclusion of ratios of permittivity, viscosity and resistivity of the fluid to that of the nanofluid.

2. MATHEMATICAL FORMULATION

In the present study, the flow of non-Newtonian (power law) electrolytic nanofluid is considered for hydrodynamically and thermally developed conditions. The flow occurs under combined action of electroosmotic force and pressure gradient. The channel is in horizontal configuration with its height being $2H$. The channel width is considered to be much larger than the channel height. It is assumed that the charge in the EDL follows the Boltzmann distribution, which happens in the case of fully dissociated symmetric salt. The electric potential distribution is found by solving Poisson's equation [21]:

$$\nabla^2\varphi = -\frac{\rho_e}{\varepsilon_{nf}} \tag{1}$$

Here ρ_e is the net electric charge density and ε_{nf} is the fluid electric permittivity. The potential φ is a combination of externally imposed field and the potential in the EDL. For an ideal solution of fully dissociated symmetric salt, the electric charge density is given by [21]

$$\rho_e = -2n_0 ez \sinh\left(\frac{ez\psi}{k_B T}\right) \tag{2}$$

where n_0 is the number ion concentration of neutral liquid, e is the charge of proton, z is the valence number of ions in the solution, k_B is the Boltzmann constant and T is the absolute temperature at a particular location.

In a fully-developed flow, EDL potential varies only in y-direction and external potential varies only in x-direction. So Eq.(1) becomes

$$\frac{d^2\psi}{dy^2} = \frac{2n_0 ez}{\varepsilon_{nf}} \sinh\left(\frac{ez\psi}{k_B T}\right) \tag{3}$$

Since for electrokinetic effects on flow through a microchannel, the temperature distribution does not affect the potential distribution much [22], the potential field and charge density can be calculated on the basis of an average temperature.

$$\frac{d^2\psi}{dy^2} = \frac{2n_0 ez}{\varepsilon_{nf}} \sinh\left(\frac{ez\psi}{k_B T_{av}}\right) \quad (4)$$

In the non-dimensional form, the Eq.(4) becomes

$$\frac{d^2\psi^*}{dy^{*2}} = \frac{2n_0 e^2 z^2}{\varepsilon_{nf} k_B T_B} H^2 \sinh(\psi^*) \quad (5)$$

where $\psi^* = \frac{ez\psi}{k_B T_B}$, $y^* = \frac{y}{H}$ and $\left(\frac{2n_0 e^2 z^2}{\varepsilon_f k_B T_{av}}\right)^{-1/2}$ is called the Debye length, denoted by λ_{Df}. The subscript *f* denotes that it is specific to the base fluid alone. The dimensionless Debye-Hückel parameter can be defined as $K = {\lambda_D}/{H}$ So Eq. (5) becomes

$$\frac{d^2\psi^*}{dy^{*2}} - \frac{\varepsilon_f}{\varepsilon_{nf}} K^2 \sinh(\psi^*) = 0 \quad (6)$$

The boundary conditions applicable are

$$\psi^*|_{y^*=1} = \zeta^* \; and \; \left.\frac{d\psi^*}{dy}\right|_{y^*=0} = 0 \quad (7)$$

where $\zeta^* = \frac{ez\zeta}{k_B T_{av}}$ is the dimensionless zeta potential.

It is assumed that the insertion of nanoparticles into the fluid has no effect on the electric double layer, nor has any interaction with it.

The flow field of the non-Newtonian electrolyte based nanofluid is governed by continuity and Cauchy momentum equations. The continuity equation in the reduced form considering steady, incompressible and fully-developed flow is

$$\frac{du}{dx} = 0 \quad (8)$$

This is because, in fully-developed condition *u* is a function of *y* alone and velocity in the *y*-direction is considered to be zero. The Cauchy momentum equation in the *x*-direction for a laminar flow becomes

$$\rho \frac{D\mathbf{V}}{Dt} = -\nabla p + \nabla . \boldsymbol{\tau} + \mathbf{F} \quad (9)$$

V is the velocity vector, *p* the applied pressure gradient, $\boldsymbol{\tau}$ the stress tensor and **F** is the body force. Here, the body force is due to the applied electric field and is given by $\rho_e E_x$, where $E_x = -d\Phi/dx$ is the electric field acting in the *x*-direction. The body force also is assumed to act only in the *x*-direction as the electric field is assumed to act in that direction only. Since velocity variation is in *y*-direction alone, the stress tensor becomes $= \mu \frac{du}{dy}$, where μ is the effective viscosity and given by

$$\mu = \mu_{0nf} \left[\left(\frac{du}{dy}\right)^2\right]^{\frac{n-1}{2}} \quad (10)$$

where μ_{nf} is the consistency index, and *n* is the flow behavior index. $n < 1$ for shear thinning fluids, $n = 1$ for Newtonian fluids and $n < 1$ for shear thickening fluids.

Applying the expressions for the terms of the momentum equation as obtained above, Eq.(9) becomes

$$\frac{d}{dy}\left\{\mu_{0nf}\left[\left(\frac{du}{dy}\right)^2\right]^{\frac{n-1}{2}} \frac{du}{dy}\right\} = \frac{dp}{dx} + 2E_x n_0 ez \sinh\left(\frac{ez\psi}{k_B T_B}\right) \quad (11)$$

To non-dimensionalize the above equation, a reference velocity has to be considered. The Helmholtz-Smoluchowski electroosmotic velocity u_{HS} has been taken as the reference velocity, which is given by

$$u_{HS} = n\lambda_{Dnf}^{\frac{n-1}{n}} \left(-\frac{\varepsilon_{nf}\zeta E_x}{\mu_{0nf}}\right)^{\frac{1}{n}} \quad (12)$$

and u_{HS} is the maximum possible electroosmotic velocity that can obtained when Debye-Hückel linearization is applied.

The nanofluid dependant properties ε_{nf} and μ_{nf} can be separated out and u_{HS} can be expressed in terms of u_{HSf} as

$$u_{HS} = n\lambda_{Df}^{\frac{n-1}{n}} \left(-\frac{\varepsilon_f \zeta E_x}{\mu_f}\right)^{\frac{1}{n}} \left(\frac{\varepsilon_f}{\varepsilon_{nf}}\right)^{\frac{n+1}{2n}} \left(\frac{\mu_{of}}{\mu_{0nf}}\right)^{\frac{1}{n}} = u_{HSf} \left(\frac{\varepsilon_f}{\varepsilon_{nf}}\right)^{\frac{n+1}{2n}} \left(\frac{\mu_{of}}{\mu_{0nf}}\right)^{\frac{1}{n}} \quad (13)$$

Another velocity u_{PD} is considered which is the maximum velocity of pressure driven flow without electrokinetic effect.

$$u_{PD}^n = \left(\frac{n}{n+1}\right)^n \left(-\frac{1}{\mu_{0nf}} \frac{dp}{dx} H^{n+1}\right) \quad (14)$$

The non-dimensional velocity u^* is given by $u^*=u/u_{HS}$. By differentiating and reducing, the left hand side of Eq.(11) can be converted to the form $nN(y^*)\frac{d^2u}{dy^2}$ where $N(y^*)=\left[\left(\frac{du^*}{dy^*}\right)^2\right]^{\frac{n-1}{2}}$. Therefore, the dimensionless momentum equation becomes

$$nN(y^*)\frac{d^2u^*}{dy^{*2}}=-\left(\frac{n+1}{n}\right)^n\Gamma\frac{\varepsilon_f}{\varepsilon_{nf}}-\frac{K^{n+1}}{n^n\zeta^*}\left(\frac{\varepsilon_f}{\varepsilon_{nf}}\right)^{\frac{n+1}{2}}\sinh\psi^* \quad (15)$$

where $\Gamma=\frac{u_{PDf}^n}{u_{HSf}^n}$

The boundary conditions are

$$\left.\frac{du^*}{dy^*}\right|_{y^*=0}=0 \quad \text{and} \quad u^*|_{y^*=1}=0 \quad (16)$$

The energy equation is written as

$$\rho c_p\frac{DT}{Dt}=\nabla.(k\nabla T)+\mu\Phi+s \quad (17)$$

where $\mu\Phi$ is the heat generation due to viscous dissipation and s is the Joule heating term given by E_x^2/σ where σ is the liquid resistivity given by $\sigma=\frac{\sigma_{0nf}}{\cosh\left(\frac{ez\psi}{k_BT_{av}}\right)}$ where σ_{0nf} is the electrical resistivity of neutral liquid.

The energy equation then becomes

$$\left(\rho c_p\right)_{nf}u\frac{\partial T}{\partial x}=k_{nf}\left(\frac{\partial^2T}{\partial x^2}+\frac{\partial^2T}{\partial y^2}\right)+\mu_{0nf}\left[\left(\frac{du}{dy}\right)^2\right]^{\frac{n-1}{2}}\left(\frac{du}{dy}\right)^2+\frac{E_x^2}{\sigma_0}\cosh\left(\frac{ez\psi}{k_BT_{av}}\right) \quad (18)$$

Let θ be the non-dimensional temperature defined as

$$\theta=\frac{T-T_w}{qH/k_{nf}} \quad (19)$$

where T_w is the wall temperature and q is the wall heat flux.

For a constant heat flux condition,

$$\frac{\partial T}{\partial x}=\frac{dT_w}{dx}=\frac{dT_m}{dx}=\text{constant} \quad (20)$$

so the axial conduction term disappears.

For steady fully-developed flow of power law nanofluid, Eq. (17) can finally be written as

$$\frac{d^2\theta}{dy^{*2}}=\left(1+S\frac{\sigma_{0f}}{\sigma_{0nf}}I_1+\frac{SS_v}{K^2}\left(\frac{\mu_{of}}{\mu_{0nf}}\right)^{\frac{1}{n}}\left(\frac{\varepsilon_f}{\varepsilon_{nf}}\right)^{\frac{-(n+1)^2}{2n}}I_2\right)\frac{u^*}{u_m^*}-\frac{SS_v}{K^2}\left(\frac{\mu_{of}}{\mu_{0nf}}\right)^{\frac{1}{n}}\left(\frac{\varepsilon_f}{\varepsilon_{nf}}\right)^{\frac{-(n+1)^2}{2n}}N(y^*)\left(\frac{du^*}{dy^*}\right)^2-$$

$$S\frac{\sigma_{0f}}{\sigma_{0nf}}\cosh\psi^* \quad (21)$$

$$S_v=\frac{\mu_{of}\sigma_{0f}u_{HSf}^{n+1}}{E_x^2\lambda_{Df}^2H^{n-1}},\ S=\frac{E_x^2H}{q\sigma_{0f}},\ u_m^*=\int_0^1u^*dy^*,\ I_1=\int_0^1\cosh\psi^*dy^*,\ I_2=\int_0^1N(y^*)\left(\frac{du^*}{dy^*}\right)^2dy^* \quad (22)$$

The boundary conditions are

$$\left.\frac{d\theta}{dy^*}\right|_{y^*=0}=0 \quad \text{and} \quad \theta|_{y^*=1}=0 \quad (23)$$

The heat transfer rates are expressed in the form of Nusselt number which can be reduced to

$$Nu=\frac{hD_h}{k_{nf}}=-\frac{4}{\theta_m} \quad (24)$$

where θ_m is the bulk mean temperature of the fluid.

Equations (6), (15) and (21) are solved numerically using the tri-diagonal matrix algorithm. Central difference scheme is applied to the equations.

$$\psi_{i+1}^*-\left(2+K^2(\Delta y^*)^2\Lambda_i^g\frac{\varepsilon_f}{\varepsilon_{nf}}\right)\psi_i^*+\psi_{i-1}^*=0 \quad (25)$$

$$u_{i+1}^*-2u_i^*+u_{i-1}^*=-\frac{(\Delta y^*)}{nN_i^g}\left[\left(\frac{n+1}{n}\right)^n\Gamma\frac{\varepsilon_f}{\varepsilon_{nf}}+\frac{K^{n+1}}{n^n\zeta^*}\left(\frac{\varepsilon_f}{\varepsilon_{nf}}\right)^{\frac{n+1}{2}}\sinh\psi^*\right] \quad (26)$$

$$\theta_{i+1}-2\theta_i+\theta_{i-1}=$$

$$(\Delta y^*)^2\left(1+I_1S\frac{\sigma_{0f}}{\sigma_{0nf}}+I_2\frac{SS_v}{K^2}\left(\frac{\mu_{of}}{\mu_{0nf}}\right)^{\frac{1}{n}}\left(\frac{\varepsilon_f}{\varepsilon_{nf}}\right)^{\frac{-(n+1)^2}{2n}}\right)\frac{u_i^*}{u_m^*}-\frac{SS_v}{4K^2}\left(\frac{\mu_{of}}{\mu_{0nf}}\right)^{\frac{1}{n}}\left(\frac{\varepsilon_f}{\varepsilon_{nf}}\right)^{\frac{-(n+1)^2}{2n}}N_i{}^g(u_{i+1}^*-u_{i-1}^*)^2-$$

$$S\frac{\sigma_{0f}}{\sigma_{0nf}}(\Delta y^*)^2\cosh\psi^* \quad (27)$$

$\Lambda_i^g = \frac{\sinh \psi_i^*}{\psi_i^*}$ and N_i^g change the non-linear system of governing equations into linear system of difference equations. These values are set after each iteration till the error obtained of the order of 10^{-8}. To evaluate the integrals Trapezoidal method is used.

3. RESULTS AND DISCUSSION

It was seen that the nanofluid behavior can be accounted for by changing three ratios, namely: viscosity ratio, $\frac{\mu_{of}}{\mu_{0nf}}$; permittivity ratio, $\frac{\varepsilon_f}{\varepsilon_{nf}}$; and resistivity ratio, $\frac{\sigma_{0f}}{\sigma_{0nf}}$. The subscript *f* indicates base fluid and *nf* denotes nanofluid. However, the three ratios $\frac{\varepsilon_f}{\varepsilon_{nf}}$, $\frac{\mu_{of}}{\mu_{0nf}}$, $\frac{\sigma_{0f}}{\sigma_{0nf}}$ do not affect the heat transfer in the same manner. Figure (1), (2) and (3) show the effect of the individual ratio (by setting the other two ratios equal to 1) on the temperature profile for Newtonian (n=1), shear thickening (n>1) and shear thinning fluids (n<1) respectively. It is seen that each particular ratio reduces the dimensionless temperature difference between the wall and centerline in the fully-developed state in all the three cases. Besides, the effect of the resistivity ratio and viscosity ratio becomes dominant for n = 1, while for the other two cases, the permittivity ratio dominates.

The effect of the change in viscosity ratio on the Nusselt number is shown in Fig. (4) for three different flow behavior index, n, keeping the permittivity and resistivity ratios as unity. Viscosity ratio affects only the temperature profile in the order of $\frac{1}{n}$ and has no effect on the velocity and EDL profile. It can be seen that as the Nusselt number decreases with decreasing viscosity ratio. Most nanofluids have a viscosity higher than that of the base fluid. So the increase in nanofluid viscosity due to increased particle concentration, has a tendency to reduce the effective heat transfer. For n=1, the exponential order for the viscosity ratio becomes unity and a straight line is obtained. However, for n=0.5, the viscosity ratio gets squared and the variation of Nusselt number with viscosity ratio becomes parabolic.

Figure (5) illustrates the effect of the ratio of permittivity on the Nusselt number at different flow behavior index. Permittivity ratio affects all the three governing equations, occurring in the order of 1 in the equation for the EDL profile, of 1 in the pressure component of the velocity profile, of $\frac{n+1}{2}$ in the electroosmotic component and in the order of $\frac{-(n+1)^2}{2n}$ in the temperature profile. It is seen that there is a rapid initial decrease in Nusselt number and then the curve flattens out with increase in the permittivity ratio when n=0.5. For n=1 and n=1.2, the curves are close to one another. This shows the effect of permittivity ratio is maximum in case of shear thinning liquids.

In Fig. (6), the effect of resistivity ratio on Nusselt number has been plotted. Resistivity of the nanofluid is less than that of the base fluid in most cases, and hence, analysis was conducted for the resistivity ratio ranging from 1 to 2. Like the viscosity ratio, the resistivity ratio affects only the energy equation. It is observed that there is a considerable increase in Nusselt number with increasing the resistivity ratio in all the three cases. It is also seen that the slope of the curves become steeper with increase in n.

The analyses were also carried out by neglecting the viscous dissipation. The results obtained are shown in Fig. (7) and (8). When viscous dissipation is not considered, the variation in Nusselt number due to permittivity and resistivity ratios are very different from those obtained by considering viscous dissipation. Hence it can be seen that both Joule heating and viscous dissipation exert considerable influence on the heat transfer behaviour.

Taking a particular case of a nanofluid, where $\frac{\varepsilon_f}{\varepsilon_{nf}} = 0.7$, $\frac{\mu_{of}}{\mu_{0nf}} = 0.8$, $\frac{\sigma_{0f}}{\sigma_{0nf}} = 1.2$, the analysis was carried out to see how it affects the Nusselt number. The values of S, S_v, ζ, Γ and K were taken as found in the work by Babaie et al. [15]. The results for base fluid can be obtained by setting the three ratios equal to 1. The results have been tabulated in Tables (1) through (3). Figure (9) illustrates the effect of the nanofluid on the variation of Nusselt number with n for various values of Γ. In all the cases, an increase in Nusselt number was observed.

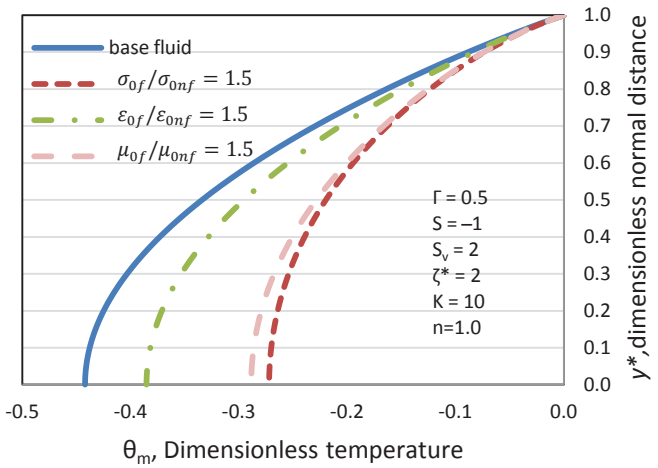

Figure 1: Effect of the individual ratios on the temperature profile for n=1

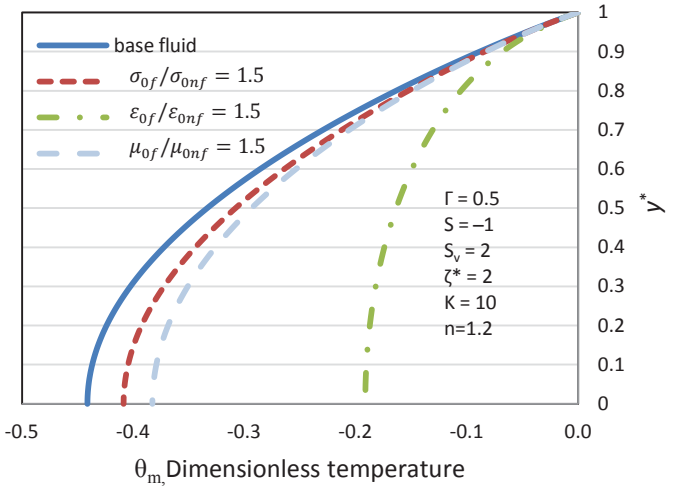

Figure 2: Effect of the individual ratios on the temperature profile for n=1.2

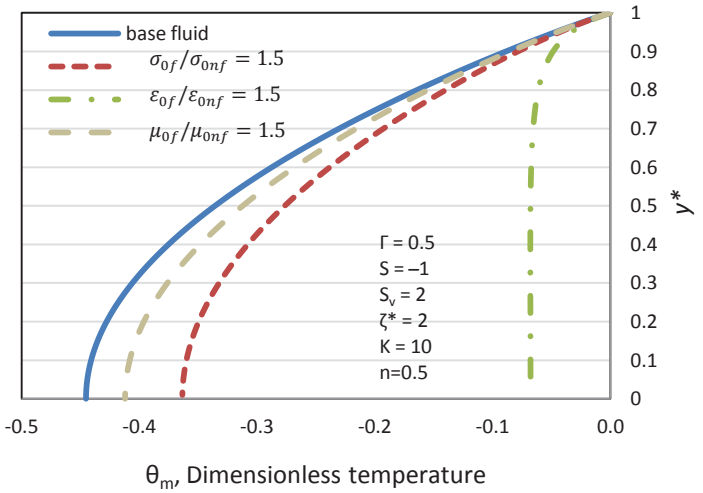

Figure 3: Effect of the individual ratios on the temperature profile for n=0.5

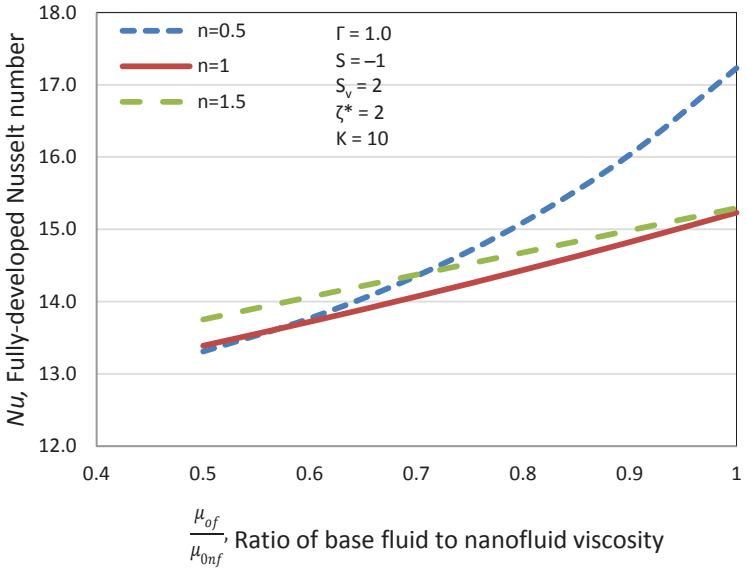

Figure 4: Variation of *Nu* with viscosity ratio with $\frac{\varepsilon_f}{\varepsilon_{nf}} = \frac{\sigma_{0f}}{\sigma_{0nf}} = 1$

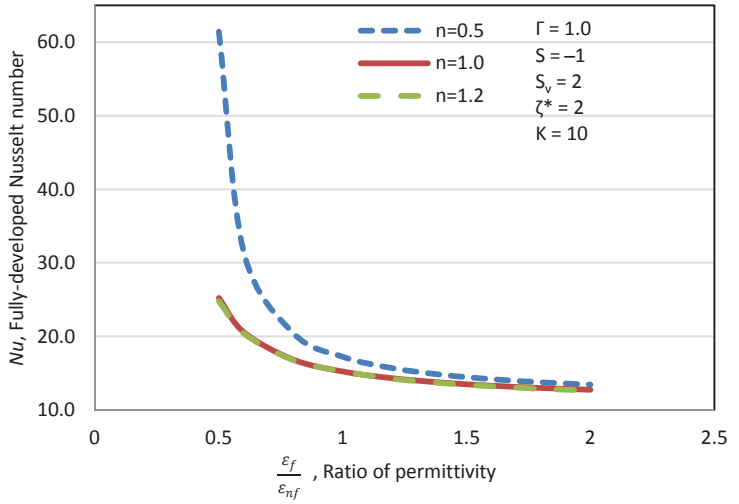

Figure 5: Variation of *Nu* with permittivity ratio keeping ratio of viscosity, $\frac{\mu_{of}}{\mu_{0nf}}$, and ratio of resistivity, $\frac{\sigma_{0f}}{\sigma_{0nf}}$, as 1

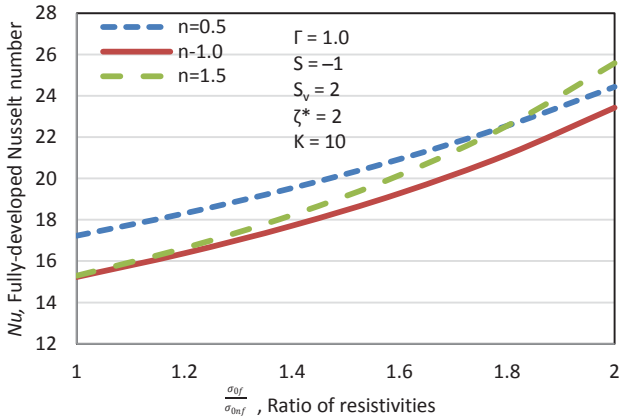

Figure 6: Variation of *Nu* with resistivity ratio with viscous dissipation with $\frac{\mu_{of}}{\mu_{0nf}} = \frac{\varepsilon_f}{\varepsilon_{nf}} = 1$

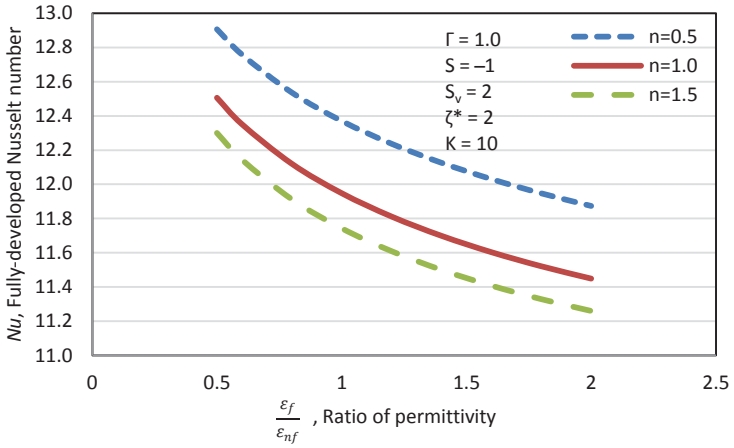

Figure 7: Variation of *Nu* with permittivity ratio without considering the effects of viscous dissipation $\left(\frac{\mu_{of}}{\mu_{0nf}} = \frac{\sigma_{0f}}{\sigma_{0nf}} = 1\right)$

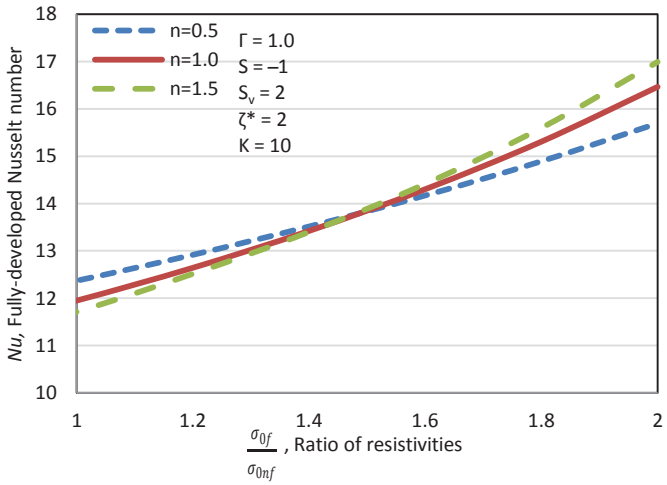

Figure 8: Variation of *Nu* with resistivity ratio with no viscous dissipation with $\frac{\mu_{of}}{\mu_{0nf}} = \frac{\varepsilon_f}{\varepsilon_{nf}} = 1$

Table 1: Difference in *Nu* with variation in *S* with and without nanofluid

S	Nusselt Number with base fluid	Nusselt number with nanofluid	% increase
-5	21.50793	24.88323	15.69328
-3	14.78057	15.91038	7.643887
-1	11.25894	11.69366	3.861109
0	10.06043	10.3254	2.633784
1	9.09254	9.24379	1.663452
3	7.62531	7.64263	0.227138
5	6.56581	6.57426	0.128697

Table 2: Difference in *Nu* with variation in S_v with and without nanofluid

S_v	Nusselt Number with base fluid	Nusselt number with nanofluid	% increase
0	14.02686	14.73601	5.055658
1	14.37356	15.23992	6.027456
2	14.73782	15.77951	7.068142
4	15.5247	16.98206	9.387363
6	16.40035	18.83016	14.8156
8	17.38067	20.03591	15.27697
10	18.48565	22.0154	19.09454

Table 3: Difference in *Nu* with variation in dimensionless zeta potential, ζ*, with and without nanofluid

ζ*	Nusselt Number with base fluid	Nusselt number with nanofluid	% increase
0	13.62143	14.053	3.168316
1	13.76234	14.26076	3.621622
2	14.24273	14.98383	5.203356
3	15.48425	16.63275	7.417214
4	17.51827	20.59074	17.53866

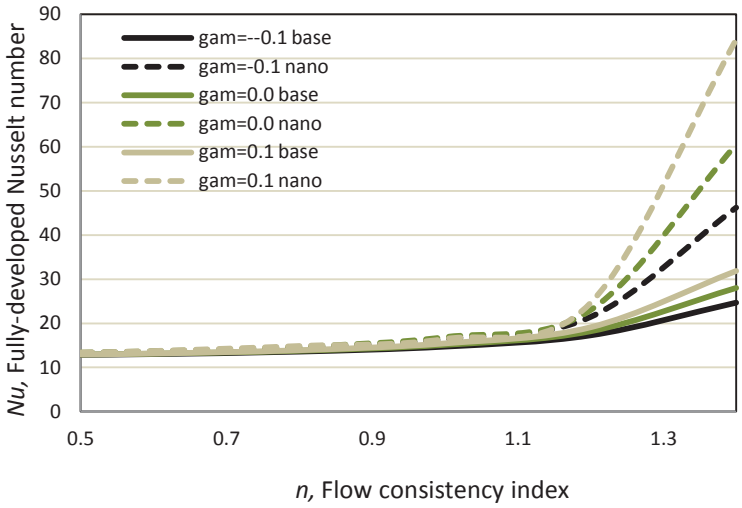

Figure 6: Effect of *n* on the fully developed Nusselt number, *Nu* for various values of Γ

5. CONCLUSIONS

A numerical analysis of the heat transfer characteristics for combined electroosmotic and pressure driven flow of non-Newtonian, electrolyte based nanofluid was carried out. It is seen that the nanofluid behavior can be accounted for by changing three thermophysical property ratios, namely: viscosity ratio $\left(\frac{\mu_{of}}{\mu_{0nf}}\right)$, permittivity ratio $\left(\frac{\varepsilon_f}{\varepsilon_{nf}}\right)$, and resistivity ratio $\left(\frac{\sigma_{0f}}{\sigma_{0nf}}\right)$. The subscript *f* indicates base fluid and *nf* denotes nanofluid. The individual effect of each ratio was studied by setting the other two ratios equal to 1. It was seen that

- Nusselt number decreases with decreasing viscosity ratio.
- Nusselt number decreases with increasing permittivity ratio.
- Nusselt number increases with increasing resistivity ratio.

Since it does not give the complete picture of the overall heat transfer characteristics of nanofluids, the analysis was extended further to conmpare the difference between the cases where $\frac{\varepsilon_f}{\varepsilon_{nf}} = \frac{\mu_{of}}{\mu_{0nf}} = \frac{\sigma_{0f}}{\sigma_{0nf}} = 1$ (simulating the base fluid) and $\frac{\varepsilon_f}{\varepsilon_{nf}} = 0.7$, $\frac{\mu_{of}}{\mu_{0nf}} = 0.8$, $\frac{\sigma_{0f}}{\sigma_{0nf}} = 1.2$ (simulating a nanofluid). It is further observed that for all fixed values of non-dimensional constants, such as, *S, S*$_v$, ζ, Γ and *K*, the Nusselt number increases with incorporation of nanofluid properties.

REFERENCES

[1] Hunter, R.J. (1981). *Zeta Potential in Colloid Science*, Academic Press, New York.
[2] Sobhan, C.B., & Peterson, G.P. (2008). *Microscale and Nanoscale Heat Transfer,* CRC Press (Taylor & Francis)
[3] Mayens, D., & Webb, B.W. (2003). Fully-developed electroosmotic heat transfer in microchannels, *Int. J. Heat Mass Transfer*, **46**, 1359-1369.

[4] Liechty, B.C., Webb, B.W., & Maynes, R.D., (2005). Convective heat transfer characteristics of electro-osmotically generated flow in microtubes at high wall potential, *Int. J. Heat Mass Transfer*, **48**, 2360-2371.

[5] Chen, C.H. (2009). Thermal transport characteristics of mixed pressure and electro-osmotically driven flow in micro- and nanochannels with Joule heating, *J. Heat Transfer*, **131**, 022401.

[6] Sadeghi, A., & Saidi, M.H. (2010). Viscous dissipation effects on thermal transport characteristics of combined pressure and electroosmotically driven flow in microchannels, *Int. J. Heat Mass Transfer*, **53,** 3782-3791

[7] Chakraborty, S. (2007). Electroosmotically driven capillary transport of typical non-Newtonian biofluids in rectangular microchannels, *Anal. Chim. Acta*, **605**, 175-184.

[8] Zhao, C., Zholkovskij, E., Masliyah, J.H., & Yang, C. (2008). Analysis of electroosmotic flow of power-law fluids in a slit microchannel, *J. Colloid Interface Sci.*, **326**, 503-510.

[9] Bharti, R.P., Harvie, D.J.E., Davidson, M.R. (2009). Electroviscous effects in fully-developed flow of a power-law liquid through cylindrical microchannel, *Int. J. Heat Fluid Flow*, **30**, 804-811.

[10] Vasu, N., & De, S. (2010). Electroviscous effects in purely pressure driven flow and stationary plane analysis in electro-osmotic flow of power-law fluids in slit microchannel, *Int. J. Eng. Sci.*, **48**, 1641-1658.

[11] Babaie, A., Sadeghi, A., Saidi, M.H. (2011). Combined electroosmotically and pressure driven flow of power law fluids in a slit microchannel, *J. Non-Newtonian Fluid Mech.*, **166,** 792-798.

[12] Das, S., & Chakraborty, S. (2006). Analytical solutions for velocity, temperature and concentration distribution in electroosmotic microchannel flows of a non-Newtonian biofluid, *Anal. Chim. Acta*, **599**, 15-24.

[13] Sadeghi, A., Fattahi, M., Saidi, M.H. (2011). An approximate analytical solution for electro-osmotic flow of power-law fluids in a planar microchannel, *J. Heat Transfer*, **133**, 091701.

[14] Chen, H.C. (2011). Electro-osmotic heat transfer of non-Newtonian fluid flow in microchannels, *J. Heat Transfer,***133**, 071705-071711.

[15] Babaie, A., Saidi, M.H., Sadeghi, A. (2012). Heat transfer characteristics of mixed electroosmotic and pressure driven flow of power-law fluids in a slit microchannel, *Int. J. Thermal Sciences*, **53**, 71-79.

[16] Choi, S. (1995). Enhancing thermal conductivity of fluids with nanoparticles, *ASME Fed.*, **231**, 99-103.

[17] Yu,W., & Choi, S.U.S. (2004). The role of interfacial layers in the enhanced thermal conductivity of nanofluids: A renovated Hamilton-Crosser model, *J. Nanoparticle Res.*, **6**, 355-361.

[18] Hung, Y.M. (2010). Analytical study on forced convection of nanofluids with viscous dissipation in microchannels, *Heat Transfer Eng.,* **31:14,** 1184-1192.

[19] Jang, S.P., & Choi, S.U.S. (2006). Cooling performance of a microchannel heat sink with nanofluids, *Appl. Thermal Eng.,* **26**, 2457-2463.

[20] Chakraborty, S., & Roy, S. (2008). Thermally developing electroosmotic transport of nanofluids in microchannels, *Microfluid Nanofluid*, **4**, 501-511.

[21] Probstein, R.F. (1994). *Physiochemical Hydrodynamics*, Second Edition, Wiley, New York.

[22] Yang, C., Li, D., & Masliyah, J.H. (1998). Modeling forced convection in rectangular microchannels with electrokinetic effects, *Int. J. Heat Mass Transfer*, **41**, 4229-4249.